THE DOWNWASH DISTRIBUTION BEHIND A WING WITH AN ANGLE OF ATTACK DISCONTINUITY AT SUPERSONIC SPEEDS

Thesis by

Welko E.Gasich

In Partial Fulfillment of the Requirements for the

Degree of Aeronautical Engineer.

California Institute of Technology
Pasadena, California.
June, 1948

ACKNOWLEDGEMENT

I wish to thank Dr. P. A. Lagerstrom for his assistance and guidance in the work to be presented and Mr. Ernest Pritchard for his fine cooperative spirit in working with the author as research colleague, and my wife for her patience in helping prepare the original manuscript.

TABLE OF CONTENTS.

1. INTRODUCTION

The stimulus for the research contained in this thesis was initiated because of a specific problem encountered by the armed forces in the field of guided missiles of the canard type. The supersonic flow field behind the missile control surfaces is investigated in order to evaluate the downwash at the lifting surfaces. This type of problem is amenable to the conical flow-theory as conceived by Busemann and later extended and applied by Lagerstrom. Lagerstrom's successful extension of this theory to the downwash problem in a supersonic flow field is utilized in this thesis.

Although it is possible to develop expressions for the downwash at all points in the wake of the control surfaces, the calculations were carried out only for the downwash field in the plane of the control surfaces.

II SUMMARY

Investigation of the downwash field behind a wing with an angle of attack discontinuity at supersonic speeds by use of linearized conical flow theory has shown the downwash to be of finite magnitude at all points in and behind the plane of the wing. The downwash at more than five chord lengths behind the wing was found to asymptotically approach the value of downwash calculated in the Trefftz plane. Behind the wing and within the span that is determined by the intersection of the Mach cones from the leading edge with the trailing edge, an unexplicable action of the downwash was found to exist. It was found that at the trailing edge the downwash was a 100 percent of that on the wing surface. At two chord lengths, the downwash was 83 percent. Upon moving aft, it was found that the downwash increased in magnitude and that at 10 chord lengths, it asymptotically approached the value at the Trefftz plane, namely 100 percent again.

By considering an idealized missile configuration, it was found that roll reversal was possible. The possibility of reversal was found to be almost entirely dependent upon the location of the control lifting surfaces with respect to one another.

A brief reference to the sidewash field was made, since the values of sidewash were a natural outgrowth of the solution of the downwash field in the Trefftz plane. An elementary consideration of the sidewash field also showed a contribution to an induced rolling moment that tends to produce roll reversal.

III NOTATION.

The system of coordinates and symbols is to be the same as that used in Reference 1 wherever possible. As pointed out in Reference 1, this system was chosen because of its adaptability to conical flow problems.

It can be seen in Figure 1 that the rectangular wing, defined by

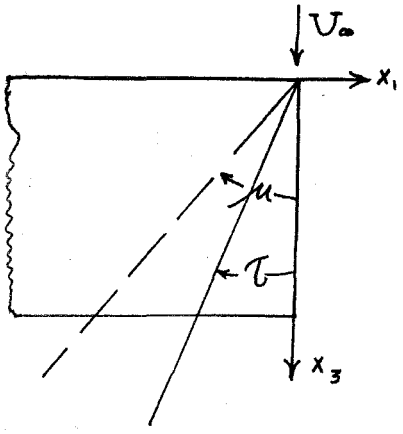

x_1 and x_3 axes , lies in the $x_1 x_3$- plane, and that the free stream velocity, is directed along the x_3-axis. The x_2-axis is vertically upwards from the $x_1 x_3$-plane. The semi-vertex angle μ is the Mach angle, and the angle τ is the angle of an arbitrary ray emanating from the vertex and lying in the plane of the wing.

Basic Coordinate System

In the theory, the wing is actually at an angle of attack and could not lie in the $x_1 x_3$ plane; but as linearization holds throughout, this difference is negligible.

The following is a list of symbols used:

$b = \frac{\tan\beta}{\tan\mu} = \frac{x_1}{m x_3}$ (denotes side edge of wing)

$B = \frac{1-\sqrt{1-b^2}}{b}$

C = Wing chord

G = Downwash function

$m = \tan\mu = \frac{1}{\sqrt{1-M^2}}$

M = Free stream Mach number

$t = \frac{x_1}{m x_3}$

$T = \frac{1-\sqrt{1-t^2}}{t}$

$t^* = \frac{t_{x_1/cm} - b}{x_3/c - 1}$

U_∞ = Free stream velocity

u_1 = Perturbation velocity in x_1 - direction

u_2 = Perturbation velocity in x_2- direction (upwash)

u_3 = Perturbation velocity in x_3-direction

α = Angle of attack

β = Arctan $\frac{x_1}{x_3}$ (angle of side edge of any superimposed wing with x_3- axis).

$\varepsilon = -\frac{u_2}{\alpha U_\infty}$ = Downward deflection angle of flow

τ = Arctan $\frac{x_1}{x_3}$

μ = Mach angle = arctan m

IV. BASIC PROBLEM.

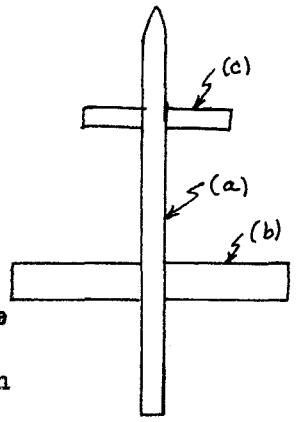

Consider the canard type missile which is shown schematically in figure 1. to be composed of three major components: (a) missile body (b) lifting surfaces and (c) roll control surfaces which operate differentially with respect to one another, ie.,when right hand surface is at $+\alpha$ the left hand side is at $-\alpha$.

Free-flight tests of a self-propelled missile of this type have shown that when the roll control surfaces are deflected to roll the missile in an arbitrary direction, say clockwise about its longitudinal axis, that due to some phenomenon the missile rolls in the opposite direction, (counter-clockwise). This reversal of control may be due to the fact that the downwash at the lifting surfaces causes an asymmetrical loading on them which produces a rolling moment of greater magnitude and opposite direction to that produced by the roll-control surfaces. The resulting motion is then opposite to that which is desired.

It is the intent of this thesis to investigate this problem from the theoretical standpoint. It will be necessary to make a further simplification in the configuration of the missile by considering the body diameter to be vanishingly small since it is beyond the scope of this paper to consider interference effects between the body and the two surfaces. The problem then resolves itself into one in which we have a wing with a discontinuous angle of attack at its midspan with a lifting wing several chord lengths behind it.

V GENERAL THEORY

In building up the theory for downwash in a supersonic flow field Lagerstrom has not used any of the concepts upon which subsonic theory is based, eg., lifting line, vortex system etc. A new approach is made to the problem by using the pressure distribution over the body as derived by linearized supersonic theory in conical flow. Since all solutions arise from a linearized theory it is evident that individual solutions to simple problems may be added in order to build up complicated flow problems. The restricting element placed upon the superposition of solutions will be met only by satisfying the boundary conditions in the flow field. It is upon this basic idea that the complete downwash theory is based. The one boundary condition that must be met at all times is that the lift is zero everywhere outside of the lifting surface. From the linearized theory considerations this implies that the velocity perturbation, u_3, in the free stream direction is also zero. The perturbation u_2, on the wing is constant and is equal to $-\alpha U_\infty$ while off the wing it is completely unrestricted and it is the object of this investigation to determine the downwash distribution behind and in the plane of the wing.

As in reference 1, this will be done by the superposition of an infinite number of auxillary wings of constant lift distribution to satisfy the boundary conditions. These auxillary wings will be formed by the superposition of two basic types of wings.

The first basic type is the infinite flat plate of zero thickness. From small perturbation theory, on the upper surface of the wing and outside of the Mach cone from the leading edge:

$$u_3 = \alpha U_\infty m$$
$$u_2 = -\alpha U_\infty \qquad (1)$$

Inside the Mach cone the values are given by:

$$u_3 = \alpha U_\infty m \arccos(1+2t) \quad (a)$$
$$u_2 = -\alpha U_\infty \quad (b) \qquad (2)$$

μ always positive

τ negative on the wing

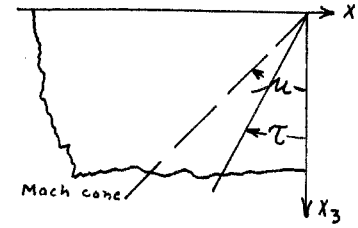

Figure 1. Lifting Quadrant

The second basic type is the conical wing of constant lift distribution as shown in figure 2. This wing is also of zero thickness; but it is not completely flat. The section of the wing which is outside the Mach cone from apex A behaves exactly as the two dimensional wing, ie., the induced velocities are determined by equations (1a) and (1b). For any point in the $x_1 x_3$- plane not within the Mach cone from A and not on the wing $u_2 = o$ and $u_3 = o$. Since by definition this is a wing of constant lift distribution then u_3 must be constant inside the Mach cone and equal to $\alpha U_\infty m$. This necessitates that u_2 become a complicated function of the wing geometry and Mach number and as pointed out in reference 1 the basic expression for the vertical velocity perturbation within the Mach cone is as follows

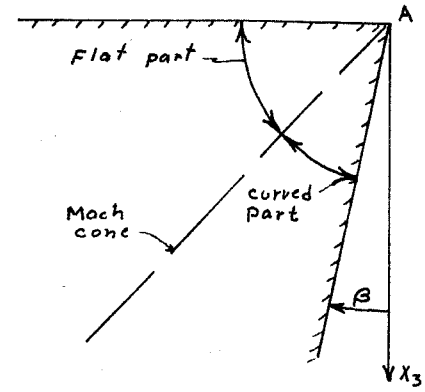

Figure2. Wing of constant lift

$$u_2 = \frac{u_3}{m\pi}\left[\frac{1}{b}\ln|T| + 2\arctan T + \frac{B^2+1}{2B}\ln\left|\frac{T-B}{1-BT}\right| - \frac{\pi}{2}\right] \qquad (3)$$

$$= \frac{u_3}{m} G(b,t)$$

where

$$b = \frac{\tan\beta}{\tan\mu}, \quad B = \frac{1-\sqrt{1-b^2}}{b}, \quad T = \frac{1-\sqrt{1-t^2}}{t}$$

It is thus seen that since u_2 is not constant on the surface of the wing within the Mach cone, the local angle of attack must vary and thus the surface must be curved in order that equations (1b) and (3) are compatible.

VI. CONSIDERATION OF THE SPECIFIC PROBLEM

We turn now to the problem of evaluating the flow field behind a finite wing with a discontinuity in angle of attack at its midspan. In general this wing will be built up in the following manner: We will just take a flat plate lifting quadrant of half infinite span to the right. Adjacent to this surface we will place a surface that will not violate the imposed boundary conditions set by wing I, as shown in fugure (3), next we will subtract wings of constant lift distribution with their leading edges at the trailing edge of the lifting quadrant in order to obtain a two dimensional wing with a discontinuity in angle of attack at midspan equal to $2\alpha_0$, as shown in figure 4.

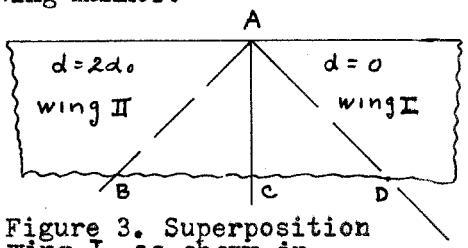

Figure 3. Superposition

From this solution we will subtract a wing of infinite span at $\alpha = +\alpha_0$. This leaves us a wing of infinite span with a wing I at $\alpha = \alpha_0$ and wing II at $\alpha = -\alpha_0$. To obtain the final result we need only to cut off the span at the desired point and superimpose upon our last solution the effect of a rectangular wing tip as given in reference 1. We then have the flow field for finite span wing with a discontinuity $\alpha = 2\alpha_0$ in angle of attack at midspan.

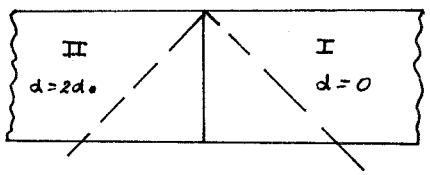

Figure 4:
Two dimensional wing with discontinuity in angle of attack.

Consider now each step of the above mentioned procedure in detail. It is seen on figure 3 that the Busemann solution for pressure on wing II (Mach cone ABC) does not apply because it could cause an upwash in the Mach cone from A in region ACD. This violates the boundary condition that the downwash in this region should be αU_∞. What is required here is the solution for a wing at an angle of attack $2\alpha_0$ in the presence of a flat plate at zero angle of attack. The solution for tip AC is obtained by

considering the solution for the tip of a non-lifting rectangular wing with a symmetrical wedge-shaped profile of half angle λ, where

$$u_3 = \frac{\lambda U_\infty m}{\pi} \arccos(t)$$

A consideration of the boundary conditions finds that they are satisfied in the following manner: the non-lifting quadrant induces no downwash in region ACD because of anti-symmetry considerations of u_2 (reference 1). Since u_3 is symmetrical on wing II, u_3 need not be zero, consequently because of the condition of no downwash in region ACD, a flat plate at $\alpha = 0$ may be introduced here without changing the flow characteristics. Since this plate prevents any flow through it, the upper surface of the wedge may be modified without altering the flow on the lower side. In particular the top side of the wedge may be removed thus leaving a lifting quadrant at $\alpha = 2\alpha_0$ in the presence of a flat plate at $\alpha = 0$, hence our spanwise distribution of pressure across the Mach cone from A may be expressed as follows:

$$u_3 = \frac{2\alpha_0 U_\infty m}{\pi} \arccos(t) \qquad (4)$$

We must now operate upon this lifting quadrant in a satisfactory manner, such that we will obtain a wing of <u>finite chord</u> as shown in figure 5. Comparing the wing, (figure 5) with the lifting quadrant, (figure 3) we see that the latter does not satisfy the boundary conditions for the former behind the trailing edge QPR. For the wing, behind QPR the streamwise velocity perturbation $u_3 = 0$ since there is no lifting surface to sustain a pressure differential. This boundary condition is violated by the lifting quadrant where u_3 is given by formula 5. In order to cancel this lift we superpose wings of constant lift distribution with their leading edges along the trailing edge QRP. These wings have no effect upstream of QRP since we are dealing with a supersonic flowfield,

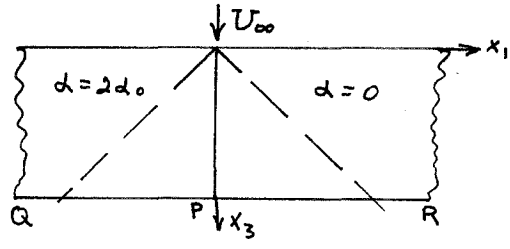

Figure 5. Wing of finite chord.

hence formula (5) is valid across the wing between Mach cones emanating from O. Since the lift varies as an arcosine function in the Mach cone, infinitely many wings of constant lift distribution are needed for cancelling the lift behind the trailing edge. As pointed out in reference 1, one first has to determine the strength, position and shape of the wings to be superimposed. Since the pressure along any ray from O,

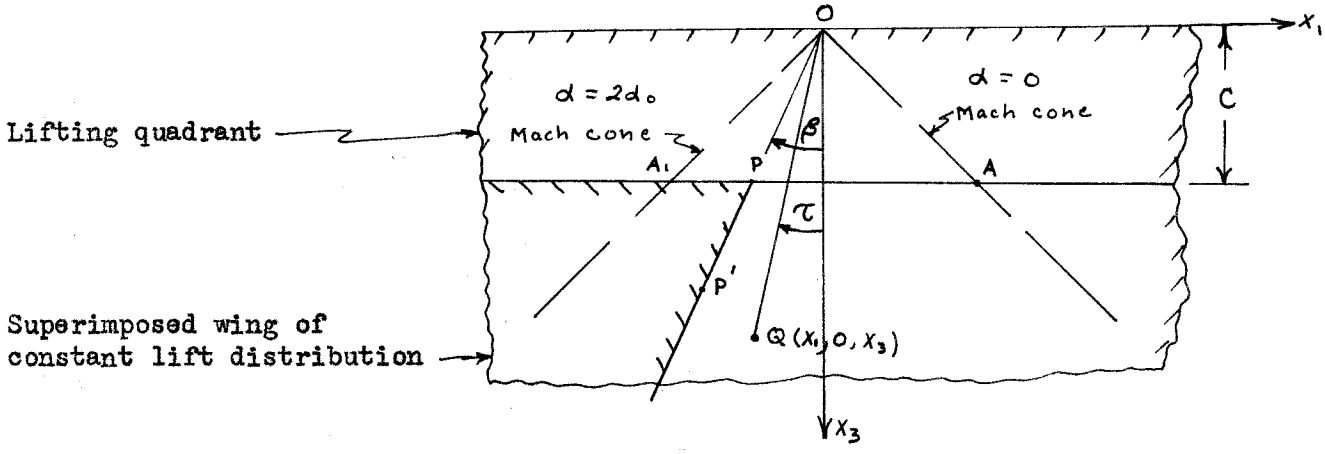

Figure 6. Superposition of wings of constant lift.

say OPP' is given by $u_3 = \frac{2\alpha_0 U_\infty m}{\pi} \cos^{-1}(b)$ then the differential strength of any superimposed conical wing should be given by the function:

$$\frac{du_3}{db}\,db = \frac{-2\alpha_0 U_\infty m}{\pi} \frac{1}{\sqrt{1-b^2}}\,db \qquad (5)$$

The superposition of these infinitely many wings of differential strength will cancel the lift of the lifting quadrant behind the chosen trailing edge of the wing and thus satisfy the boundary condition that $u_3 = 0$ except on the wing itself. Hence the contribution to the downwash at a point $Q(X_1, 0, X_3)$ due to a differential wing of constant lift will be given by the following formula:

$$u_2(Q) \text{ due to wing at } P = -\frac{1}{m} G(b, t^*) \frac{du_3}{db}\,db \qquad (6)$$

where $G(b,t^*)$ is given by (3) with t^* substituted for t

and where $t^* = \frac{\frac{x_1}{cm} - b}{\frac{x_3}{c} - 1}$ since the apex of the superimposed wing is at point P and not point O from which t is measured, hence t^* is used. To this contribution must be added the downwash due to

the original lifting quadrant which is given by $u_2(Q)$ due to lifting quadrant $= \frac{1}{m} G(b,t) \frac{du_3}{db}\, db$. The total downwash at point $Q(X_1, 0, X_3)$ is given by the sum of the above two contributions and then integrating the expression from $b = +1$ to $b = -1$:

$$u_2 = \frac{1}{m} \int_{b=1}^{b=-1} \left[G(b,t) - G(b,t^*) \right] \frac{du_3}{db}\, db \qquad (7)$$

Since the integrand as given by G(b,t) is of such complicated form that it does not allow the integration to be carried out in closed form, graphical integration was used. To expedite the calculations a basic chart was used giving G(b,t) vs. t with b as a parameter. The chart, as prepared, was for values of $-1 < t < 1$ and $-1 < b < 0$). Since the range of the variable of integration, b, used in this problem varied between the values of $-1 < b < 1$ the value of G(b,t) for positive values of b may be determined by consideration of the superposition principle to give $G(b,t) = \left[-1 - G(b,t) \right]$. By choosing a given point $Q(\frac{X_1}{cm}, 0, \frac{X_3}{c})$ at which the downwash was to be obtained and knowing t and t* both G(b,t) and G(b,t*) could be found directly on the chart for various values of b. Hence a plot could be made of $\left[\frac{G(b,t) - G(b,t^*)}{d_0 U_\infty m} \right] \frac{du_3}{db}$ for various values of b from +1 to -1, and the area under this curve was the required downwash given by $\frac{-u_2}{d U_\infty}$. As pointed out in reference 1, the curve of the plotted integrand is infinite at various points and special means (as developed by Lagerstrom) were used to nullify these infinities.

The subterfuge used in the cancellation of the infinities is based upon the fact that the strength of an infinitesimal conical wing will not cause an infinite downwash; hence at any point at which the downwash function approaches an infinite value a simple rule of elementary calculus is resorted to. The following example will be used:

Consider a function f(x) which has an integrable infinity between the limits of integration. Subtract from this function a new function g(x)

which has a singularity of the same order at the point at which f(x) is singular, ie $\int_a^b \left[f(x) - g(x)\right] dx + \int_a^b g(x)\, dx$

It is obvious that the value of the total integral is still equal to the value of the original integral and at the same time the integral under the first integral sign is finite. The method of choosing the function g(x) is done (1) by inspection or (2) by expanding the original function f(x) about the point at which the singularity occurs in a Taylor series, being careful that the function itself does not become infinite.

The function $\left[G(b,t) - G(b,t^*)\right]\frac{du_3}{db}$ has singularities and indeterminacies depending upon the position $Q(\frac{x_1}{cm}, o, \frac{x_3}{c})$, hence the method of treating the singularities may be divided into three different cases: (1) $0 > \frac{x_1}{cm} > -1$, (2) $\frac{x_1}{cm} < -1$ (3) $\frac{x_1}{cm} = -1$, (Cases for positive values of $\frac{x_1}{cm}$ were not calculated because the downwash was found to be an odd function with respect to the x_1 - axis as will be pointed out later by considerations at the trailing edge).

CASE 1

The function $\left[G(b,t) - G(b,t^*)\right]\frac{du_3}{db}$, hereafter called $G(b,Q)\frac{du_3}{db}$ is infinite when $\frac{du_3}{db}$ is infinite, ie $b = \pm 1$ and is infinite when Q lies on the axis of a Mach cone from the tip of the superimposed conical wing as shown in figure 7.

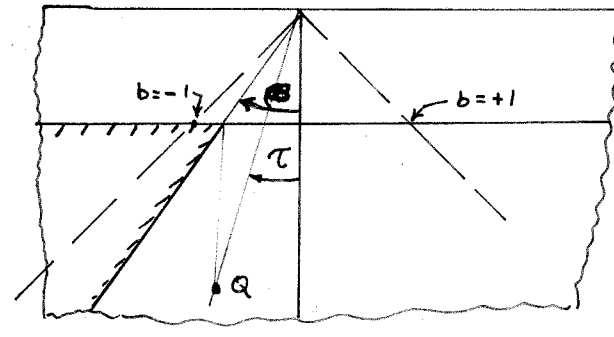

Figure 7. Superimposed conical wing.

Part A: $\frac{du_3}{db}$ infinity:

the infinity due to $\frac{du_3}{db}$ can be nullified in the following manner:

at b = -1:

$$\int_{b_1}^{-1}\left[G(b,Q)\frac{du_3}{db}\,db\right] = \int_{b_1}^{-1}\left[G(b,Q) - R\right]\frac{du_3}{db}\,db + \int_{b_1}^{-1} R\,\frac{du_3}{db}\,db \qquad (8)$$

where

$$R = \frac{1}{\pi}\left[\ln\left|\frac{T^*}{T}\right| + 2\arctan T - 2\arctan T^*\right] \qquad (9)$$

at $b = +1$:

$$\int_{b_2}^{+1} G(b,Q)\frac{du_3}{db}\,db = \int_{b_2}^{+1}\left[G(b,Q) - S\right]\frac{du_3}{db}\,db + \int S\frac{du_3}{db}\,db \qquad (10)$$

where

$$S = \frac{1}{\pi}\left[\ln\left|\frac{T}{T^*}\right| + 2\arctan T - 2\arctan T^*\right] \qquad (11)$$

Part B: G(b,Q) infinity:

For the case when G(b,Q) is infinite, ie when $b = \frac{x_1}{cm}$ ($T^* = 0$) the removal of the infinity is made in the same manner as for the case of a rectangular wing tip as developed in reference 1, in the following manner:

$$\int_{b_3}^{b_4} G(b,Q)\frac{du_3}{db}\,db = \int_{b_3}^{b_4}\left[G(b,Q)\frac{du_3}{db} - h(b)\right]db + \int_{b_3}^{b_4} h(b)\,db$$

where

$$h(b) = \frac{1}{\pi\frac{x_1}{cm}}\left(\frac{du_3}{db}\right)_{b=\frac{x_1}{cm}}\left[\left(\frac{x_1}{cm} - b\right)\ln\left|\frac{x_1}{cm} - b\right| - \left(\frac{x_1}{cm} - b\right)\right] \qquad (12)$$

and

$$G(b,Q)\frac{du_3}{db} - h(b) = \left(\frac{du_3}{db}\right)_{b=\frac{x_1}{cm}}\frac{1}{\pi}\left\{\frac{1}{x_1/cm}\left(\ln T + \ln 2\left(\frac{x_3}{c} - 1\right) + \frac{\sqrt{1-\left(\frac{x_1}{cm}\right)^2}}{x_1/cm}\left[\ln|B| - \ln\left|\frac{T-B}{1-BT}\right|\right] + 2\arctan T\right)\right\} \qquad (13)$$

CASE II: $\frac{x_1}{cm} < -1$

$G(b,Q)\frac{du_3}{db}$ is infinite when $\frac{du_3}{db}$ is infinite ($b = \pm 1$) as was shown in Case 1. G(b,Q) is indeterminate, that is both (G(b,Q) and G(b,t) become infinite when $b = t = t^*$. This occurs when Q lies on the edge of a superimposed conical wing and an original wing, each of which produces a line of infinite downwash along its edge.

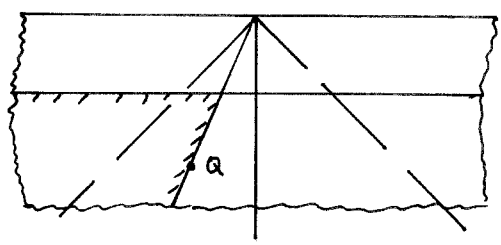

Figure 8. Point Q on edge of conical wing.

Evaluating G(b,Q) at $b = t = t^*$:

$$G(b,Q) = \frac{1}{\pi}\left[\frac{1}{b}\ln\left|\frac{T}{T^*}\right| + 2(\arctan T - \arctan T^*) + \frac{B^2-1}{2B}\ln\left|\frac{T-B}{1-BT}\,\frac{1-BT^*}{T^*-B}\right|\right]$$

$$\underset{b=t^*}{G(b,Q)} = \frac{1}{\pi}\,\frac{B^2-1}{2B}\ln\left|\frac{T-B}{T^*-B}\right|$$

Taking the limit of the argument of the logarithm

$$\lim_{t^*\to b}\left[\frac{T-B}{T^*-B}\right] = \frac{-dB/db}{\frac{dT^*}{dt^*}\frac{dt^*}{db} - \frac{dB}{db}}$$

Since

$$\frac{dB}{db} = \frac{B}{b\sqrt{1-b^2}}, \qquad \frac{dT^*}{dt^*} = \frac{T^*}{t^*\sqrt{1-t^{*2}}}$$

and

$$\frac{dt^*}{db} = \frac{d}{db}\left(\frac{\frac{x_1}{cm} - b}{\frac{x_3}{c} - 1}\right) = \frac{-1}{\frac{x_3}{c} - 1}$$

then

$$\lim_{t^x \to b}\left[\frac{T-B}{T^x-B}\right] = \frac{\dfrac{B}{b\sqrt{1-b^2}}}{\dfrac{T^x}{t^x\sqrt{1-t^{x2}}}\dfrac{1}{\frac{x_3}{c}-1} - \dfrac{B}{b\sqrt{1-b^2}}} = -\frac{\frac{x_3}{c}-1}{x_3/c}$$

hence

$$\underset{b=t^x=t_b}{G(b,Q)} = \frac{1}{\pi}\frac{\sqrt{1-t_b^2}}{t_b}\ln\left|\frac{x_3/c}{x_3/c-1}\right|$$

CASE III ($\frac{x_1}{cm} = -1$)

This case is similar to Case 1 except that the term $\frac{du_3}{db}$ also becomes infinite when G(b,Q) becomes infinite, that is G(b,Q) is infinite when $b = \frac{x_1}{cm} = -1$ which is one of the roots at which $\frac{du_3}{db}$ is infinite: Thus we have a double infinity when b = -1. In order to subtract out this double infinity, G (b,Q) and L are introduced as follows:

In the interval b_o to -1,

$$\frac{1}{m}\int_{b_o}^{-1} G(b,Q)\frac{du_3}{db}\,db = -\frac{2d_oU_\infty}{\pi}\int_{b_o}^{-1}\left[\frac{1}{\sqrt{1-b}}G(b,Q) - \frac{1}{\sqrt{2}\,\pi}\ln|1+b| - L_S\right]\frac{db}{\sqrt{1+b}}$$

$$-\frac{2d_oU_\infty}{\pi^2\sqrt{2}}\int_{b_o}^{-1}\frac{\ln(1+b)}{\sqrt{1+b}}\,db - \frac{2d_oU_\infty}{\pi}\int_{b_o}^{-1}\frac{L_S}{\sqrt{1+b}}\,db$$

Let:

$$\bar{G}_s(b,Q) = \frac{1}{\sqrt{1+b}}G(b,Q) - \frac{1}{\sqrt{2}\,\pi}\ln|1+b|$$

and

$$L_S = \bar{G}_s(-1,Q) = \frac{1}{\sqrt{2}\,\pi}\left\{-\ln|T| + 2\arctan T + \lim_{b\to -1}\ln\left|\frac{T^x}{1+b}\right|\right\}$$

as $b \to -1$, $T^x \to \frac{t^x}{2} \to 0$ where $t^x = \frac{-1-b}{x_3/c-1}$; $\lim_{b\to -1}\ln\left|\frac{T^x}{1+b}\right| = \ln\lim\left|\frac{\frac{-1-b}{2(x_3/c-1)}}{1+b}\right| =$

$$= -\ln 2\left(\frac{x_3}{c}-1\right)$$

Therefore:

$$L_S = \frac{1}{\pi\sqrt{2}}\left\{-\ln|T| + 2\arctan T - \ln 2\left(\frac{x_3}{c}-1\right)\right\}$$

Although $\frac{\bar{G}_s(b,Q)-L_s}{\sqrt{1+b}}$ is indeterminant for b = -1, it may be shown by expanding it in a power series, that

$$\lim_{b\to -1}\frac{\bar{G}_s(b,Q)-L_s}{\sqrt{1+b}} = 0$$

Since it is finite for b = -1,

$$-\frac{2d_oU_\infty}{\pi}\int_{b_o}^{-1}\left[\frac{1}{\sqrt{1-b}}G(b,Q) - \frac{1}{\pi\sqrt{2}}\ln|1+b| - L_S\right]\frac{db}{\sqrt{1+b}}$$

is integrated graphically.

$$-\frac{2d_oU_\infty}{\sqrt{2}\,\pi^2}\int_{b_o}^{-1}\frac{\ln|1+b|}{\sqrt{1+b}}\,db = -0.546\,d_oU_\infty \quad \text{, for } b_o = -.50$$

$$-\frac{2d_oU_\infty}{\pi}\int_{b_o}^{-1}\frac{L_S}{\sqrt{1+b}}\,db = 0.900\,d_oU_\infty L_S \quad \text{, for } b_o = -.50$$

Now we can write:

$$(u_2)_{\frac{x_1}{c_m}=-1} = \frac{1}{m}\int_{1}^{-1} G(b,Q)\frac{du_3}{db}\,db \equiv \frac{1}{m}\int_{.5}^{-.5} G(b,Q)\frac{du_3}{db} - \frac{2\alpha_0 U_\infty}{\pi}\int_{-.5}^{-1}[\bar{G}_s(b,Q)-L_s]\frac{db}{\sqrt{1+b}}$$

$$-\frac{2\alpha_0 U_\infty}{\sqrt{2}\,\pi^2}\int_{-.5}^{-1}\frac{\ln|1+b|}{\sqrt{1+b}}\,db - \frac{2\alpha_0 U_\infty}{\pi}\int_{-.5}^{-1}\frac{L_s}{\sqrt{1+b}}\,db + \frac{1}{m}\int_{1}^{.5}[G(b,Q)-S]\frac{du_3}{db} + \frac{1}{m}\int_{1}^{.5} S\frac{du_3}{db}\,db$$

Where, as before:

$$S = \frac{1}{\pi}\left[\ln\left|\frac{T}{T^x}\right| + 2\arctan T - 2\arctan T^x\right]_{b=1}$$

and

$$\frac{1}{m}\int_{1}^{.5} S\frac{du_3}{db} = \frac{2\alpha_0 U_\infty m S}{m\pi}\left[\arccos(b)\right]_{1}^{.5} = .667\,\alpha_0 U_\infty S$$

The first, second and fifth terms of the above expression are integrated graphically.

Figure 9 shows a typical case in which singularities are encountered three times in the range of integration of G(b,Q) across the Mach cone. The chart of G(b,t) vs t with b as a parameter was used. Calculations were then completed by means of tables, see Table 1. By plotting the final value obtained vs b and integrating by using a planimeter the integral for a specific ray angle, t = - 0.2 in this case, may be obtained. Figure 9 shows how the artifice of subtracting a suitable function from $G(b,Q)\frac{du_3}{db}$ is used at b = +1 and b = -1 where $\frac{du_3}{db}$ is infinite, which was explained for part A, Case 1. At $b = -.4 = \frac{x_1}{c_m}$ an example of Part B, Case 1 is illustrated as discussed in Case II. Adding to the planimetered area, the integrated value of the subtracted functions gives the downwash equal to 0.836 for this point Q(-0.4, 0, 2). Calculations were carried out in this manner for points at 2, 5 and 10 chord lengths behind the wing and are presented in figure 10. Figure 11 is a cross-plot of figure 10.

DOWNWASH AT THE TRAILING EDGE

The downwash at the trailing edge may be determined analytically in the following manner: the downwash velocity is given by expression (7) as:

$$u_2 = \frac{1}{m}\int_{+1}^{-1}\left[G(b,t) - G(b,t^x)\right]\frac{du_3}{db}\,db$$

which is equivalent to

$$u_2 = -\frac{1}{m}\int_{+1}^{-1} G(b,t^x)\frac{du_3}{db}\,db + \frac{1}{m}\int_{+1}^{0} G(b,t)\frac{du_3}{db}\,db + \frac{1}{m}\int_{0}^{-1} G(b,t)\frac{du_3}{db}\,db$$

The second integral is zero since $G(b,t) = 0$ for a wing at $\alpha = 0$, while the third integral gives the two dimensional value: $G(b,t) = -1$. Hence for $0 < t < 1$

$$u_2 = \frac{1}{m}\int_1^t \frac{du_3}{db}\,db = \frac{2\alpha_0 u_\infty}{\pi}\left[u_3(t) - u_3(1)\right] = \frac{2\alpha_0 u_\infty}{\pi}\arccos(t) \qquad (15)$$

and for $-1 < t < 0$

$$u_2 = \frac{1}{m}\int_1^t \frac{du_3}{db}\,db - \frac{1}{m}\int_0^{-1} \frac{du_3}{db}\,db$$

$$= \frac{2\alpha_0 u_\infty}{\pi}\arccos t - 2\alpha_0 u_\infty = -2\alpha_0 u_\infty\left[1 - \frac{1}{\pi}\arccos t\right] \qquad (16)$$

These values are plotted on figure 10 with the downwash for several other finite chord lengths behind the wing.

DOWNWASH AT INFINITY:

The problem of computing the downwash-sidewash field in the Trefftz plane is shown in reference (1) to be the same as that in incompressible flow, and the methods of complex variables may be used.

The vortex sheet trailing back from the wing is unaltered, in the first approximation, from the trailing edge to $x_3 = \infty$, and remains in the plane of the wing. Thus the sidewash is a known function all along the x_1 axis in the Trefftz plane. $u_1 = 0$ for $\frac{x_1}{cm} < -1$ and for $\frac{x_1}{cm} > 1$ since there is no sidewash coming from the two dimensional part of the wing. Behind the region where the Mach cone intersects the trailing edge of the wing $\left(-1 \leqslant \frac{x_1}{cm} \leqslant 1\right)$ $u_1 = F\left(\frac{x_1}{cm}\right)$ at $\frac{x_2}{cm} = 0+\varepsilon$ and $u_1 = -F\left(\frac{x_1}{cm}\right)$ at $\frac{x_2}{cm} = 0-\varepsilon$ where ε is an infinitesimal distance and $\to 0$. This furnishes one boundary condition for the problem in the Trefftz plane. The other boundary condition is that u_2 vanish at $r_1 = \sqrt{\left(\frac{x_2}{cm}\right)^2 + \left(\frac{x_1}{cm}\right)^2} = \infty$.

The function $F\left(\frac{x_1}{cm}\right)$ is evaluated at the trailing edge of the wing by use of the well known formula derived from conditions of irrotational flow:

$$\frac{du_1}{dt} = -\frac{1}{mt}\,\frac{du_3}{dt} \qquad (17)$$

$u_3 = u_3(t)$ is assumed known. For the justification for this procedure, see reference (1).

It was noticed by Dr.Lagerstrom that the same boundary conditions are satisfied when a solution that vanishes on the Mach cone in the $\mathcal{E}$ plane is transformed to the physical plane by the inverted Joukowski transformation: $\mathcal{E} = \frac{1-\sqrt{1-z^2}}{z}$

$$\frac{2}{Z} = \mathcal{E} + \frac{1}{\mathcal{E}} \qquad (18)$$

where $\mathcal{E}$ and Z are complex variables.

The $\mathcal{E}$ plane here referred to is that perpendicular to the x_3 axis at $\frac{x_3}{c} = -1$ and is the one encountered in conical flow problems described in reference 3. In the $\mathcal{E}$ plane, the coordinates have been transformed from the physical plane through the Chaplygin transformation $R = \frac{1-\sqrt{1-r_1^2}}{r_1}$ to allow the use of the solutions to Laplace's equation.

It may be seen that in applying the transformation (18), the unit circle in the $\mathcal{E}$ plane transforms into the portion of the x_1 axis in the physical plane where $|x_1| \geq 1$. It is also seen that the point $r = 1$, $\theta = \frac{\pi}{2}$ in the $\mathcal{E}$ plane transforms to $\frac{x_1}{cm} = \infty$ in the physical plane. Thus the boundary conditions in the $\mathcal{E}$ plane for $u_1 - i\,u_2 = U(\mathcal{E})$ become $u_1 = 0$ on the unit circle, $u_2 = 0$ at $r=1$, $\theta = \frac{\pi}{2}$ and $U(x) = F\left(\frac{x_1}{cm}\right)$ on the x axis, where: $X = \frac{1-\sqrt{1-(x_1/cm)^2}}{x_1/cm}$

Now the procedure outlined above will be applied to the problem at hand. From reference (2):

$$u_3 = \frac{2\alpha_0 m u_\infty}{\pi} \cos^{-1}(t)$$

and by formula (17):

$$u_1 = \frac{2\alpha_0 u_\infty}{\pi} \ln\left|\frac{1+\sqrt{1-t^2}}{t}\right|$$

At the trailing edge $t = \frac{x_1}{cm}$, therefore:

$$u_1 = \frac{2\alpha_0 u_\infty}{\pi} \ln\left|\frac{1-\sqrt{1-(x_1/cm)^2}}{x_1/cm}\right| = F\left(x_1/cm\right)$$

Now using formula (18) in the $\mathcal{E}$ plane:

$$u_1 = \frac{2\alpha_0 u_\infty}{\pi} \ln(X)$$

The boundary conditions on u are obviously satisfied for:

$$u_1 - i u_2 = \frac{2\alpha_0 u_\infty}{\pi}\left[\ln(\mathcal{E}) - i\frac{\pi}{2}\right]$$

$$u_2 = \frac{\pi}{2} - \theta$$

$$u_1 = \frac{2\alpha_0 u_\infty}{\pi} \ln r$$

Thus in the ζ plane, r = constant represents lines of constant sidewash, and θ = constant represents lines of constant upwash.

It is easiest to think of the transformation $\frac{1}{z} = \frac{1}{2}\left(\zeta + \frac{1}{\zeta}\right)$ in two steps: $\frac{1}{2}\left(\zeta + \frac{1}{\zeta}\right) = \zeta_1$ and $\zeta_1 = \frac{1}{z}$. The first step is the well known Joukowski transformation, and the second is the ordinary inversion about the unit circle. From this, the formulas for the lines of constant sidewash and upwash in the physical plane turn out to be:

$$r_1^2 = \left[\frac{(2c_3)^2}{(c_3^2-1)^2}\sin^2\theta_1 + 1\right]\frac{(2c_3)^2}{(c_3^2+1)^2}$$

where: $c_3 = e^{\frac{\pi}{2}\frac{u_1}{d_0 u_\infty}}$

r_1 and θ_1 are the polar coordinates in the z (physical) plane.

$$r_1^2 = \frac{(1-c_1^2) - \sin^2\theta_1}{(1-c_1^2)c_1^2}$$

where: $c_1 = \cos\left[\left(1 - \frac{u_2}{d_0 u_\infty}\right)\frac{\pi}{2}\right]$

These are plotted in Figures (12) and 13. Figures (14) and (15), are crossplotted from Figures (12) and (13).

DISCUSSION AND RESULTS VII

The results of the graphical integration for obtaining the downwash at finite chord lengths are shown on figure 10. It is apparent that behind wing I ($\alpha = +\alpha_0$) that we have a downwash field while behind wing II ($\alpha = -\alpha_0$) we have an upwash field. It is interesting to note that at the discontinuity in angle of attack that we have a finite break in downwash. Since the upwash curves are odd functions of the parameter t for any given distance behind the wing it is apparent that we have no net downwash, thus indicating no net lift produced by the wing. This is to be expected since the angles of attack are opposite in sense. At 2,5 and 10 chord lengths behind the wing the downwash (upwash) increases in magnitude to a given value of t and then remains constant. The point at which this break in variation occurs is directly behind the point at which the Mach cone intersects the trailing edge of the wing ie. at $\frac{x_1}{c_m} = \pm 1$. For values of t corresponding to $1 > \frac{x_1}{c_m} > -1$ it is seen that the downwash is approximately -1.0 at one chord length. At two chord lengths it has decreased to -.82 and then it gradually increases again to approach -1.0 at 10 chord lengths and attains exactly -1.0 at infinity. The reason for the peculiar action of the downwash field is not fully understood. It may be due to an interchange of energy in the wake as the wake proceeds downstream.

The values of downwash of figure 10 have been cross plotted to show the positions of lines of constant downwash in figure 11. It is obvious that the major strength of the field occurs within the region directly behind the intersection of the Mach cones with the trailing edge. For the values of $\left|\frac{u_2}{\alpha_0 u_\infty}\right| > .30$ it is seen that the lines of constant downwash rapidly approach the asymptotic value that is calculated in the Trefftz plane (figure 12); hence for design purposes where the tailplane

is located at $\frac{X_2}{c} > 5$ we may use the values of $\frac{u_2}{d_\infty u_\infty}$ at infinity.

The downwash and sidewash field in the Trefftz plane is presented in figure 12. Figure 13 is a magnification of the first quadrant of figure 12. The lines of constant downwash are lemniscates, while lines of constant sidewash are ovals . For values of $-2 > \frac{X_1}{cm} > 2$ the downwash field decays rapidly in the plane of the wing ($x_2 = 0$), and when out of the plane of the wing the initial values of downwash decrease rapidly. Inspection of figure 14, which is a cross plot of figure 12, bears this point out very strongly. At $\frac{X_1}{cm} = \pm .5$ we see that the maximum downwash has dropped to fifty percent of the value in the plane of the wing. At $\frac{X_1}{cm} = \pm 1.0$ the maximum has dropped to thirty percent. These facts show good cause to the designer for placing the tail plane surfaces out of the plane of the wing.

Figure 15, which is a cross plot of 12, shows variation of sidewash in the Trefftz plane for various $\frac{X_1}{cm}$ ie out of the vertical plane. It is interesting to note that for $\frac{X_1}{cm} = .5$ that the sidewash does not decrease to zero at the origin as the downwash did when out of the plane symmetry. It is apparent that if a missile were of such a configuration that it had two vertical tail surfaces at the extremity of its horizontal surfaces that a rolling moment would be acting upon the missile due to the sidewash distribution as shown by figure 15.

Consider now the downwash field for a specific configuration of a canard-type missile, to illustrate the possibility for obtaining roll reversal as was discussed in section IV. A missile configuration as shown in figure 16 was chosen, with control surface span equal to lifting wing span with the wing located five and one third chord lengths behind the control surface. The wing chord is 25 percent greater than the control surface chord. It is important to point out that the induced rolling moment is directly proportional to the wing chord. The downwash field as deduced

in the Trefftz plane was used since it was pointed out earlier that for $\frac{x_3}{c} > 5$, the values of $\frac{u_2}{\alpha_0 u_\infty}$ at $x_3 = \infty$ could be used to a very good approximation. The downwash values from Mach cone B were those obtained in this thesis. The downwash values due to the tip Mach cones, A and C, were obtained from reference 1. By superposing the solutions we arrive at a result which shows the presence of an extremely strong upwash field behind the wing for which $\alpha = -\alpha_0$ and a strong downwash field behind the wing for which $\alpha = +\alpha_0$. The magnitudes of upwash and downwash are both greater than 100 percent of the downwash on the control surface itself. The rolling moment due to the discontinuity in angle of attack is clockwise (missile viewed from rear) while the induced rolling moment due to the downwash field is counter-clockwise, and of greater magnitude than that produced by the control surface because of the fact that $\frac{u_2}{\alpha_0 u_\infty} > 1$ at any point along the span of the wing. Thus a possibility of obtaining roll reversal is shown. The configuration used in this case was chosen so that the roll reversal would be obvious without integrating the lift across the half span of the lifting wing due to the continuously varying aerodynamic angle of attack. In general, whether roll reversal is obtained depends entirely upon the missile configuration.

VIII REFERENCES

1. P. A. Lagerstrom, M. E. Graham, "Downwash and Sidewash Induced by Three Dimensional Lifting Wings in Supersonic Flow", Douglas Aircraft Co. Report No. SM-13007, 1947.

2. P. A. Lagerstrom, M. E. Graham, "Linearized Theory of Supersonic Control Surfaces", Douglas Aircraft Co. Report No. SM-13060, 1947.

3. P. A. Lagerstrom, "Linearized Supersonic Theory of Conical Wings", Jet Propulsion Laboratory, California Institute of Technology, Progress Report 4-36, December 4, 1947.

IX TABLES AND GRAPHS

TABLE I

b	Downwash at point Q(-.4,0,2) G(b,t) G(b,t) chart	t*	G(b,t*) t* same as 2	G(b,Q)	$\frac{du_3}{db}$	$G(b,Q)\frac{du_3}{db}$
0	-2.11	-.40	-1.36	-.75	-.636	.477
-.10	-2.70	-.30	-1.81	-.89	-.639	.569
-.15	-3.38	-.25	-2.40	-.98	-.644	.631
-.20	(Indeterminate: *)			-1.08	-.650	.702
-.25	-2.11	-.15	-.89	-1.22	-.658	.804
-.30	-1.09	-.10	.35	-1.44	-.667	.960
-.35	-.62	-.05	1.25	-1.87	-.680	1.270

At the indeterminacy G(b,Q) is given by: $G(b,Q) = \frac{1}{\pi}\frac{\sqrt{1-b^2}}{b}\ln\left|\frac{x_3/c}{x_3/c - 1}\right|$

At $b = -.40 = x_1/cm$ G(b,Q) is infinite, hence part B of Case I is used to eliminate the infinity where the expression in given by equation (13):

b	T	B	2 arctan T	$\frac{x_3}{c}$	$G(b,Q)\frac{du_3}{db}$ -h(b) equation (13)
-.35	-.10	-.183	-.20	2	-.455
-.40	-.10	-.210	-.20	2	-.531
-.45	-.10	-.239	-.20	2	-.581

Integrating the subtracted function h(b), the following expression is obtained:

$$\int_{-.35}^{-.45} h(b)\frac{du_3}{db}\,db = \frac{1}{\pi\frac{x_1}{cm}}\left(\frac{du_3}{db}\right)_{b=\frac{x_1}{cm}}\left[\left(\frac{x_1}{cm}-b\right)\ln\left|\frac{x_1}{cm}-b\right| - \left(\frac{x_1}{cm}-b\right)\right]_{-.35}^{-.45}$$

$$= -.221\,d_0 U_\infty m$$

Between b = -.45 and b = -1.0, the funtion G(b,Q) -R was used because of the infinity at b = -1.0 due to the infinity in du_3/db as explained in Case I, part A:

b	G(b,t)	t*	G(b,t*)	T*	T/T* T=-.10	$\ln\left\|\frac{T}{T^*}\right\|$	B	arctg T*
-.45	-.185	.05	1.305	.026	-3.85	1.348	-.239	.026
-.50	-.078	.10	.800	.050	-2.00	.693	-.268	.050
-.60	.050	.20	.410	.100	-1.00	0	-.333	.100
-.80	.140	.40	.150	.210	-.476	-.743	-.500	.210
-.90	.158	.50	.092	.268	-.373	-.986	-.627	.262
-.95	.165	.55	.075	.300	-.334	-1.097	-.731	.292

b	2(arctan T-arctan T*)	R	G(b,Q)-R	du_3/db	G(b,Q)-R
-.45	-.152	-.477	-1.013	-.714	.724
-.50	-.300	-.316	-.562	-.736	.413
-.60	-.400	-.127	-.233	-.797	.186
-.80	-.620	.039	-.049	-1.061	.052
-.90	-.724	.084	-.018	-1.460	.026
-.95	-.784	.099	-.009	-2.040	.018

$$\underset{-b=1.0}{R} = 0.114$$

$$\int R \frac{du_3}{db}\, db = \frac{R\, 2\alpha_0 U_\infty m \arccos b}{\pi} \Big/_{b_1=-.45}^{-1.0} = +0.0815\alpha_0 U_\infty m$$

Starting with b = 0 and calculating $G(b,Q)\frac{du_3}{db}$ for positive values of b:

b	G(b,t)	t*	G(b,t*)	G(b,Q)	du_3/db	$G(b,Q)\,du_3/db$
0	-2.11	-.40	-1.36	-.75	-.636	.477
.25	-1.645	-.65	-1.078	-.567	-.658	.374
.40	-1.531	-.80	-1.023	-.508	-.695	.354
.60	-1.413	-1.00	-1.00	-.413	-.797	.330
.80	-1.350			-.350	-1.06	.371
.85	-1.325			-.325	-1.21	.394
.90	-1.317			-.317	-1.46	.462
.95	-1.305			-.305	-2.04	.621

Between b = 0.85 and b = 1.00, the function G(b,Q)-S was used as explained in Case I, part A where S is given by expression (11):

b	T	2 arctan T	T*	2 arctg T*	S	G(b,Q)-S	$[G(b,Q)-S]\frac{du_3}{db}$
.85	-.10	-.20	-1.0	-1.57	-.296	-.029	.04
.90	-.10	-.20	-1.0	-1.57	-.296	-.021	.03
.95	-.10	-.20	-1.0	-1.57	-.296	-.009	.02

$$\underset{b=+1.0}{S} = -0.296$$

$$\int_{+.85}^{+1.0} S \frac{du_3}{db} db = -0.1035 d_o U_\infty m$$

FIGURE 9. ILLUSTRATION OF GRAPHICAL METHOD OF OBTAINING UPWASH

EXAMPLE AT Q (-.4, 0, 2)

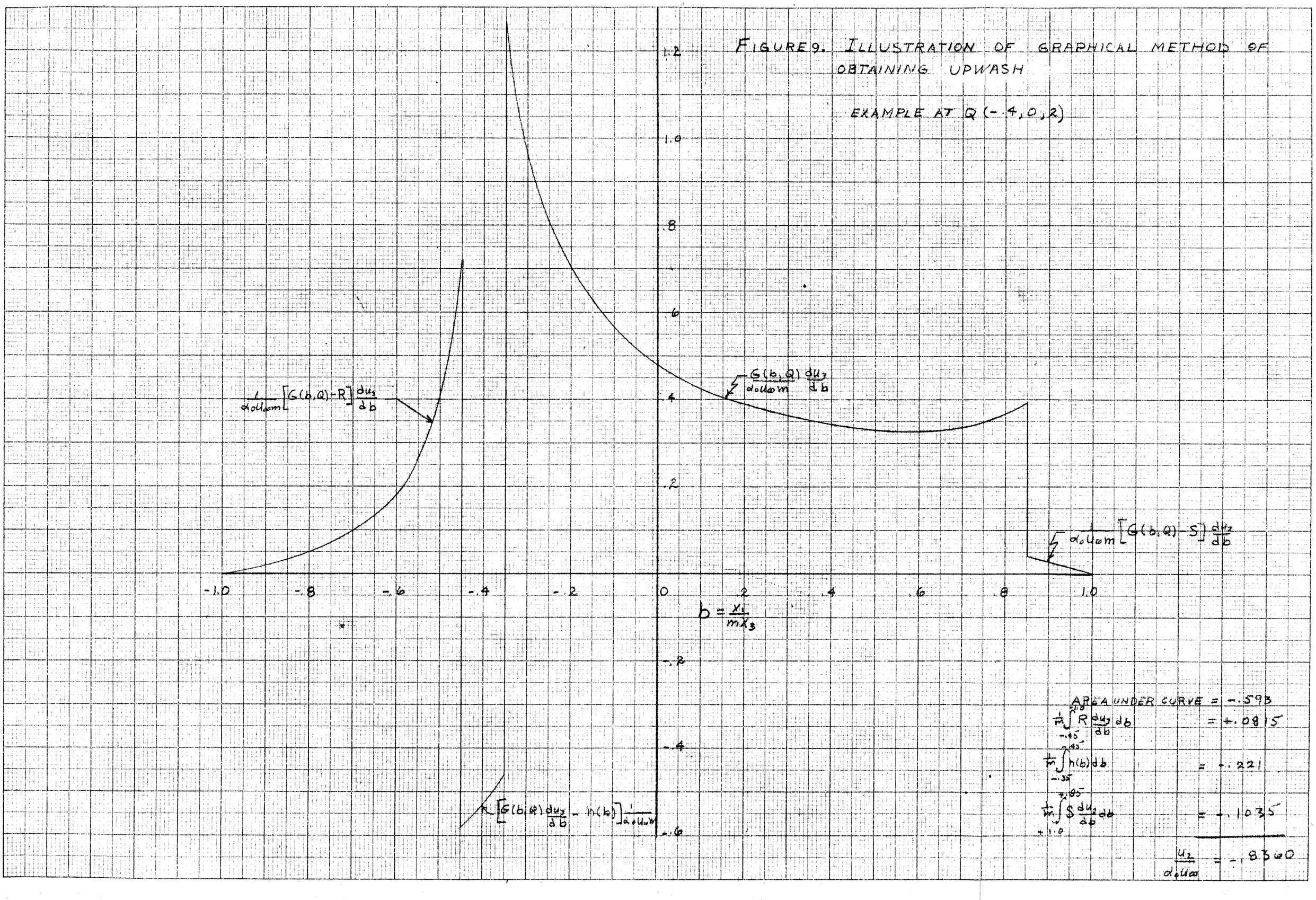

AREA UNDER CURVE = -.593

$\frac{1}{m}\int_{-1.5}^{2.0} R\frac{du_3}{db}\,db$ = +.0815

$\frac{1}{m}\int_{-1.55}^{-.45} h(b)\,db$ = +.221

$\frac{1}{m}\int_{+1.0}^{+.85} S\frac{du_3}{db}\,db$ = +.1035

$\frac{u_2}{\alpha_0 U_\infty}$ = -.8360

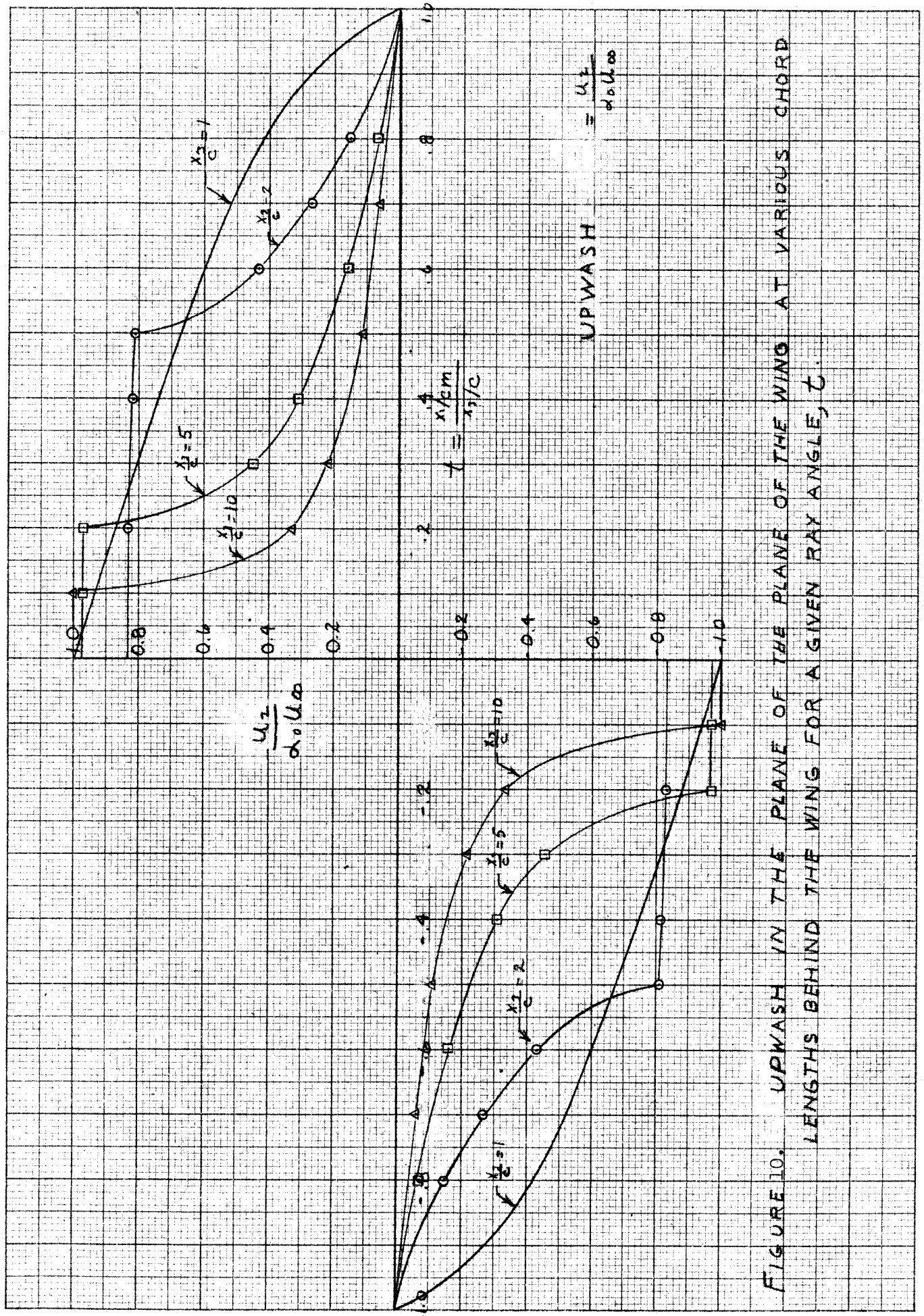

FIGURE 10. UPWASH IN THE PLANE OF THE WING AT VARIOUS CHORD LENGTHS BEHIND THE WING FOR A GIVEN RAY ANGLE, ζ.

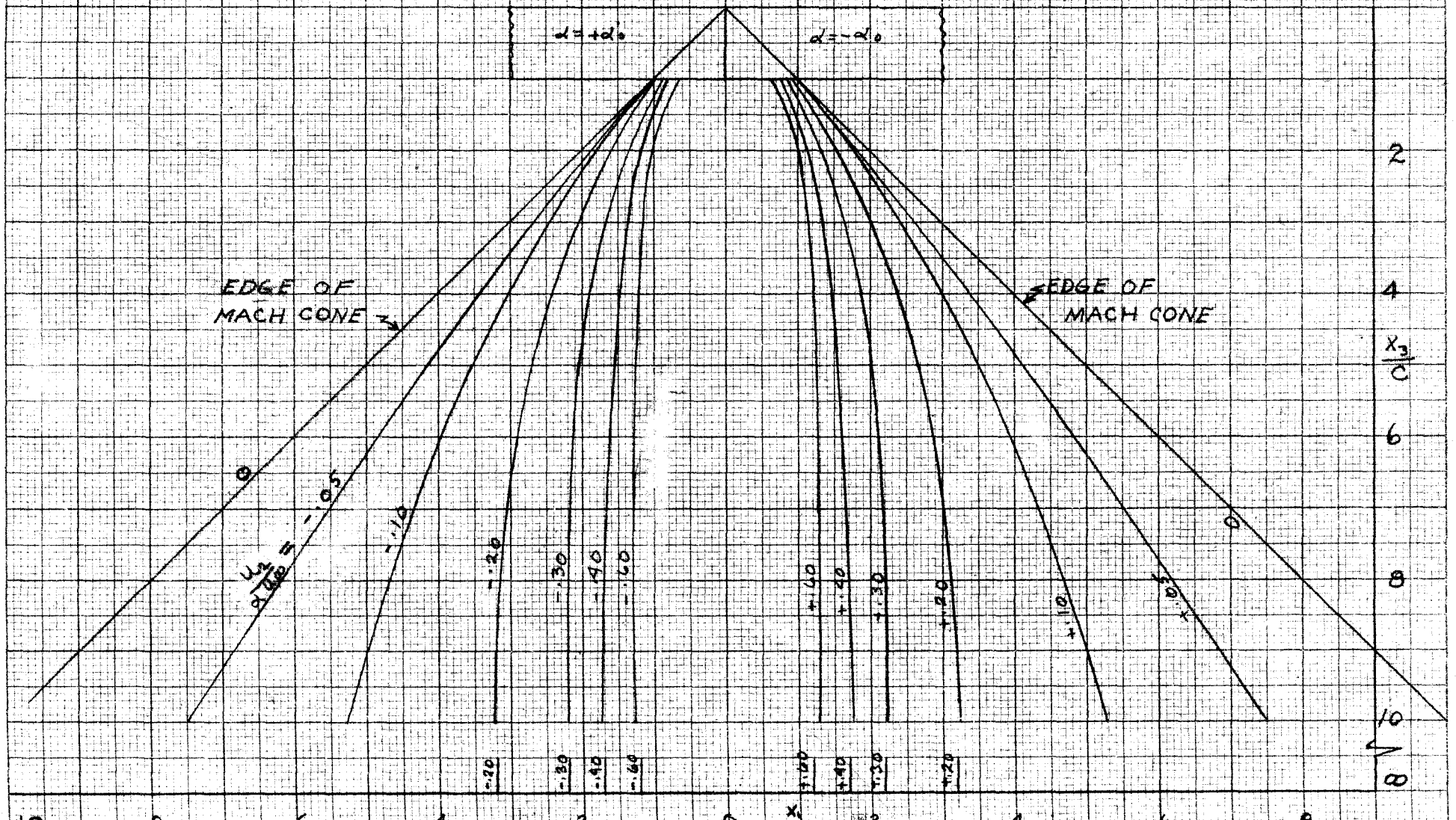

FIGURE 11. LINES OF CONSTANT UPWASH IN THE PLANE OF THE WING.

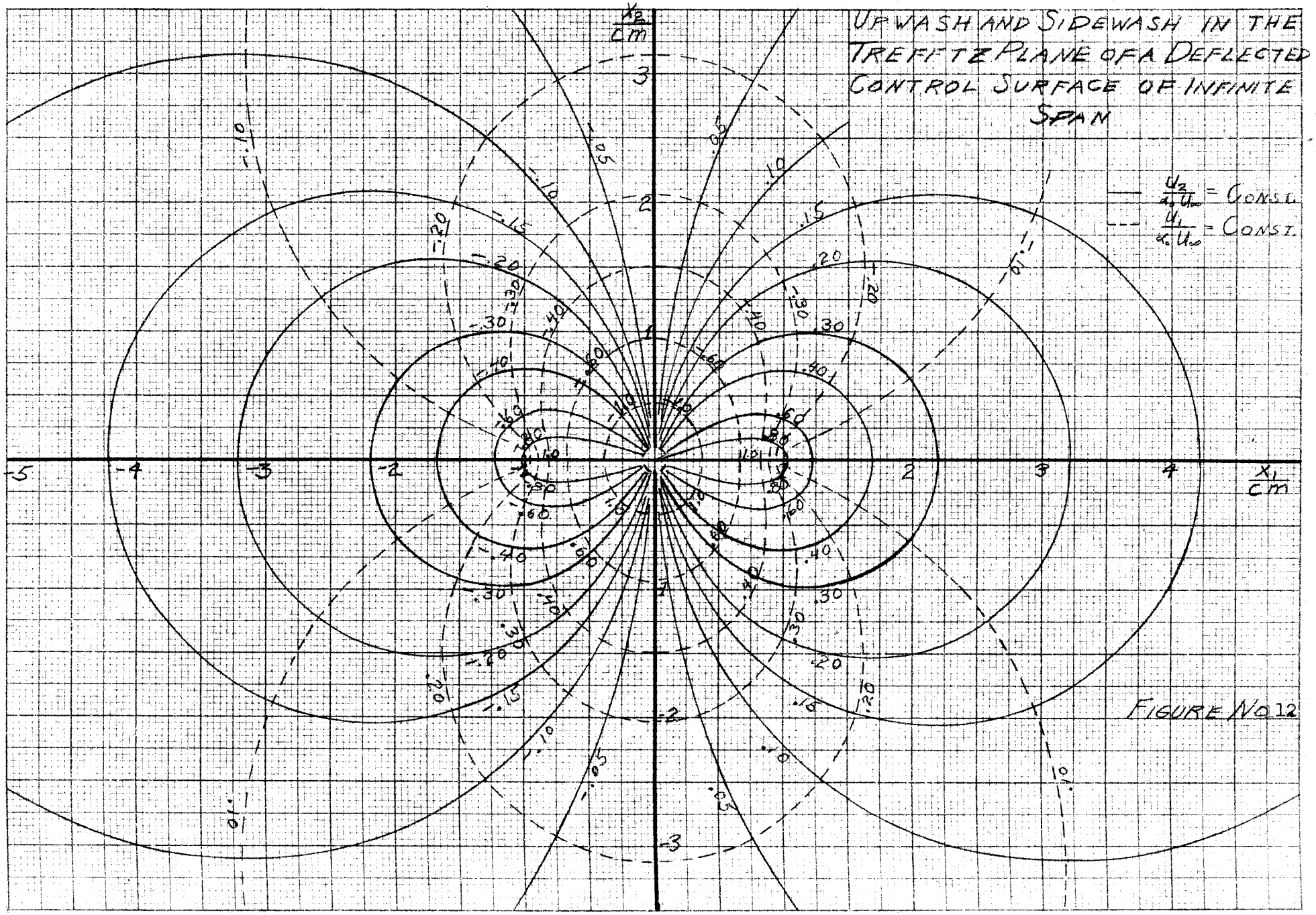
UPWASH AND SIDEWASH IN THE TREFFTZ PLANE OF A DEFLECTED CONTROL SURFACE OF INFINITE SPAN
$\frac{w_2}{\alpha_1 U_\infty}$ = CONST.
$\frac{u_1}{\alpha_1 U_\infty}$ = CONST.
$\frac{x_2}{cm}$
$\frac{x_1}{cm}$

FIGURE NO 12

UPWASH & SIDEWASH IN THE FIRST QUADRANT OF THE TREFFTZ PLANE OF A DEFLECTED CONTROL SURFACE OF INFINITE SPAN

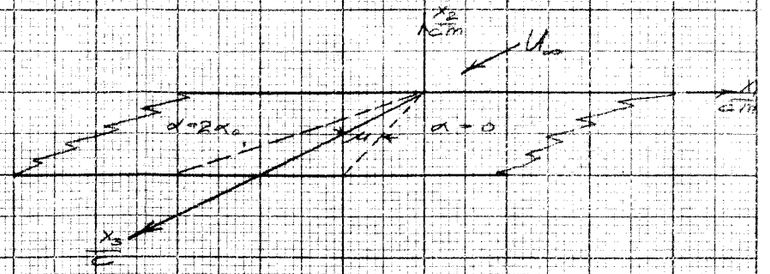

FIGURE NO. 13.

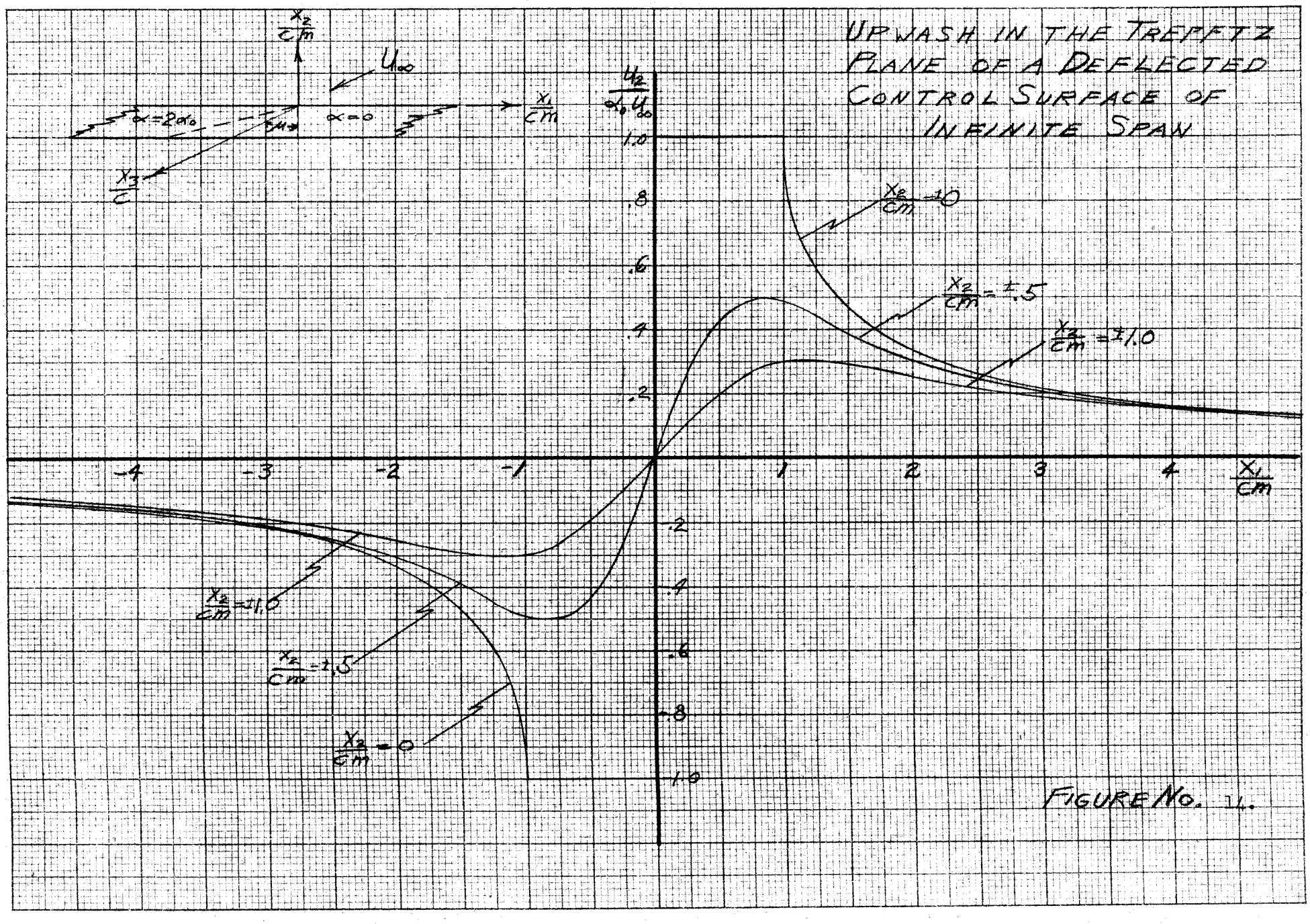
UPWASH IN THE TREFFTZ PLANE OF A DEFLECTED CONTROL SURFACE OF INFINITE SPAN
$\frac{X_2}{c_m}$
U_∞
$\alpha = 2\alpha_0$
$\alpha = 0$
$\frac{X_1}{c_m}$
$\frac{X_3}{c}$
$\frac{u_2}{\alpha_0 U_\infty}$
1.0
.8
.6
.4
.2
$\frac{X_2}{c_m} = 1.0$
$\frac{X_2}{c_m} = \pm .5$
$\frac{X_2}{c_m} = \pm 1.0$
-4
-3
-2
-1
1
2
3
4
$\frac{X_1}{c_m}$
-.2
-.4
-.6
-.8
-1.0
$\frac{X_2}{c_m} = \pm 1.0$
$\frac{X_2}{c_m} = \pm .5$
$\frac{X_2}{c_m} = 0$

FIGURE NO. 14.

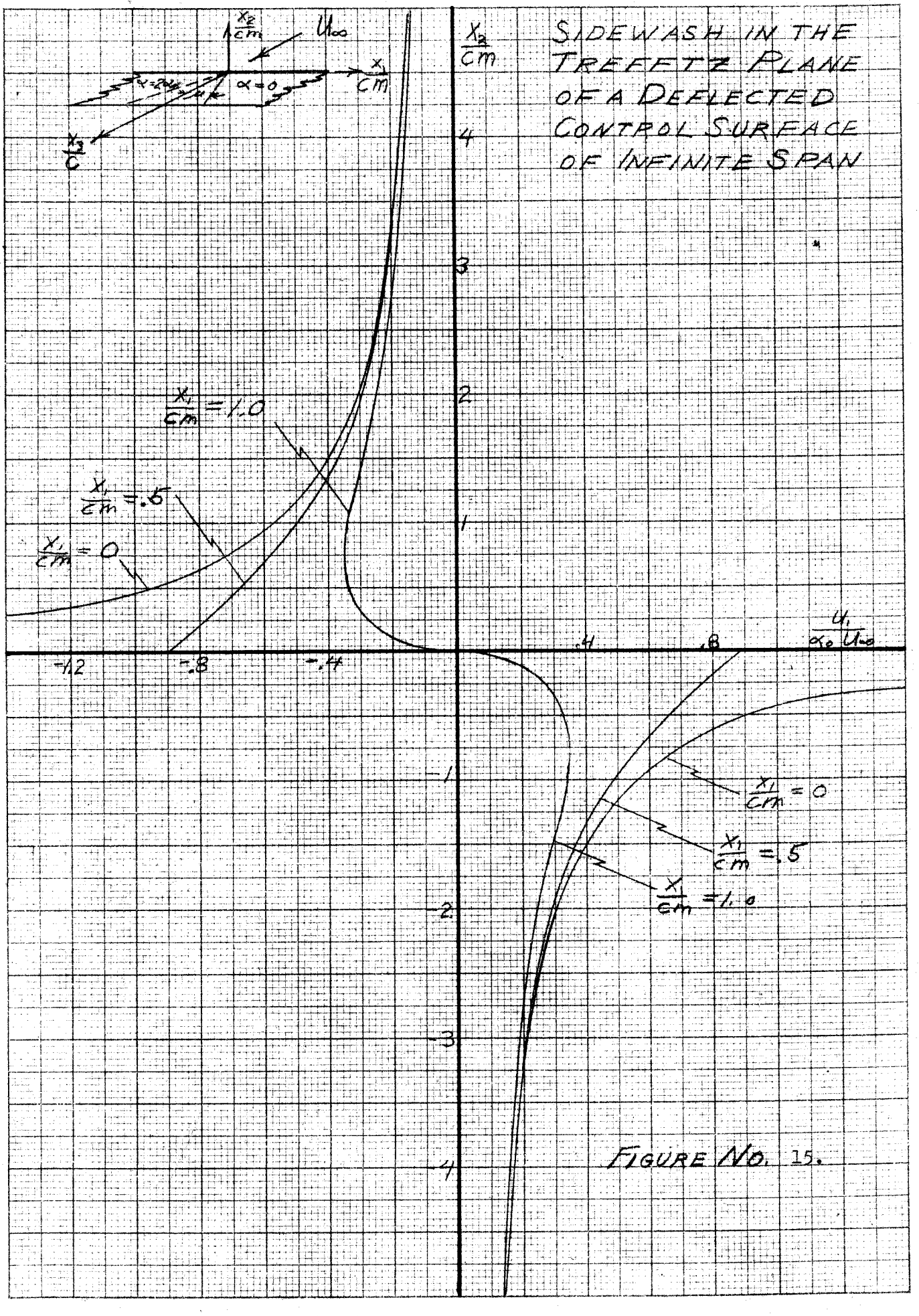
SIDEWASH IN THE TREFFTZ PLANE OF A DEFLECTED CONTROL SURFACE OF INFINITE SPAN
$\frac{x_2}{cm}$
U_∞
$\frac{x_1}{cm}$
$\alpha = 0$
$\alpha = 20°$
$\frac{x_2}{c}$
$\frac{x_1}{cm} = 1.0$
$\frac{x_1}{cm} = .5$
$\frac{x_1}{cm} = 0$
$\frac{u_1}{\alpha_0 U_\infty}$
-1.2
-.8
-.4
.4
.8
4
3
2
1
-1
-2
-3
-4
$\frac{x_1}{cm} = 0$
$\frac{x_1}{cm} = .5$
$\frac{x_1}{cm} = 1.0$

FIGURE NO. 15.

ILLUSTRATION OF ONE POSSIBILITY FOR OBTAINING ROLL REVERSAL.

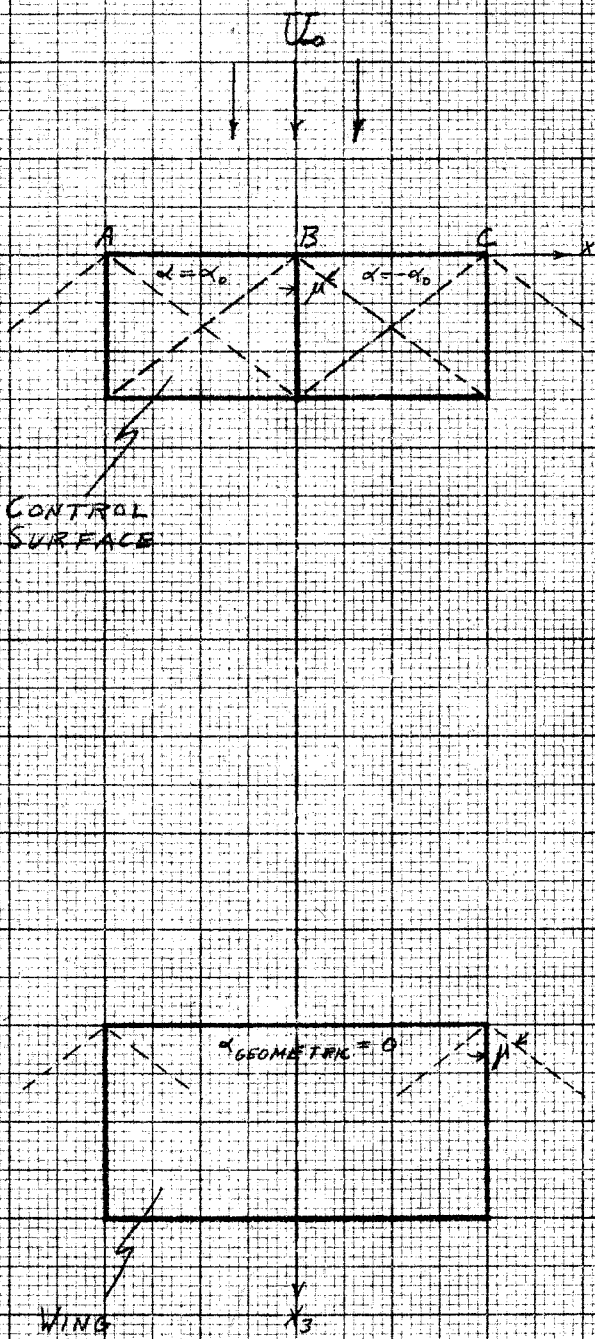

SIMPLIFIED CANARD CONFIGURATION

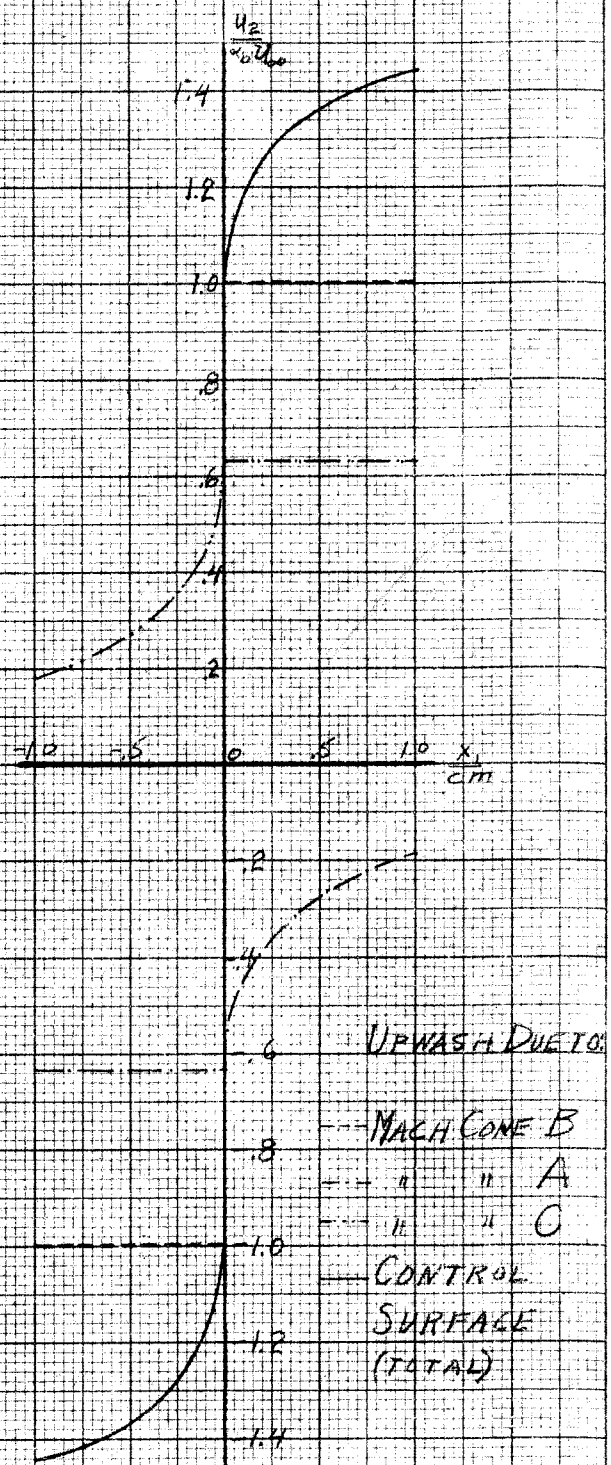

UPWASH DISTRIBUTION AT LEADING EDGE OF CANARD WING.

FIG. NO. 16.